The Generalized Valence Bond Description of the Valence States of Formamide[1,2]

Lawrence B. Harding[3] and William A. Goddard III*[2]

Contribution No. 5061 from the Arthur Amos Noyes Laboratory of Chemical Physics, California Institute of Technology, Pasadena, California 91125. *Received February 20, 1975*

Abstract: The wave functions for the valence states of formamide (NH_2CHO) are reported using ab initio generalized valence bond (GVB) and configuration interaction (GVB-CI) wave functions. The character and properties of the states are analyzed in terms of the GVB wave functions. The calculated vertical excitation energies to the $^3A''(n \rightarrow \pi^*)$, $^1A''(n \rightarrow \pi^*)$, and $^3A'(\pi \rightarrow \pi^*)$ states are 5.39, 5.65, and 6.19 eV, respectively. The only experimental result known is the $^1A''$ absorption which peaks at 5.65 eV, in excellent agreement with our results. The calculated ground state dipole moment is 3.79 D, in good agreement with the experimental value of 3.71 D. Calculated dipole moments of the $^3A'$, $^1A''$, and $^3A''$ states are 3.29, 2.19, and 2.05 D, respectively. The calculated barrier to rotation about the C–N bond is 18.2 kcal, in good agreement with the experimental liquid phase values (16–20 kcal).

I. Introduction

The basic structural unit of protein molecules is the peptide bond consisting of a carbonyl group attached to a saturated nitrogen. The most important interaction in this unit should be the interaction of the lone pair orbital on the nitrogen with the π system of the carbonyl, as occurs in formamide. As a model for the peptide bond we have carried out accurate ab initio studies of formamide.

First we will build up a qualitative description of formamide $NH_2HC{=}O$ in terms of the wave functions of formaldehyde $H_2C{=}O$ and the amide radical; $\cdot NH_2$.

In the valence bond model the valence states of formaldehyde have the form[4]

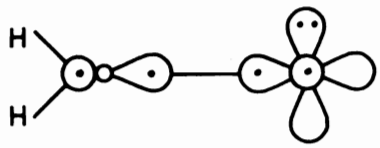

(1)

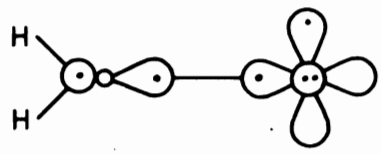

(2)

where the p orbitals parallel and perpendicular to the plane are represented by ∞ and O, respectively, and singlet pairing of two orbitals is indicated by a line joining them. Coupling the remaining singly occupied orbitals into either a singlet pair or a triplet pair leads to the $^1A_1$(ground state) or the $^3A_1(\pi\text{-}\pi^*)$ state for (1) and to the $^1A_2$ or $^3A_2(n\text{-}\pi^*)$ state for (2).

The $^2A_1$ state of NH_2 has the form

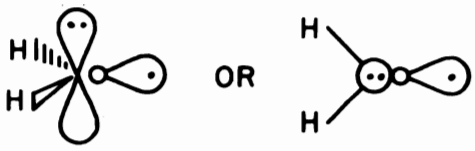

(3)

consisting of a doubly occupied π orbital and a singly occupied sp hybridized σ orbital.

Replacing a hydrogen from (1) or (2) with an NH_2 group, (3), yields the following valence states of planar formamide.

With the σ orbitals singlet paired, (4) and (5) each lead to a singlet state and a triplet state: $^1A'$ and $^3A'$ for (4) and

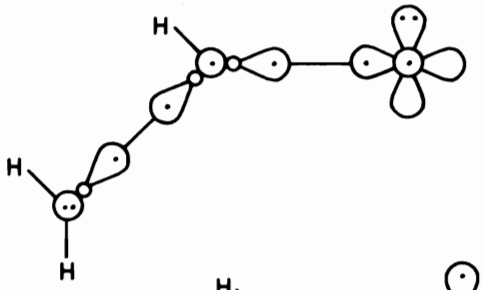

(4)

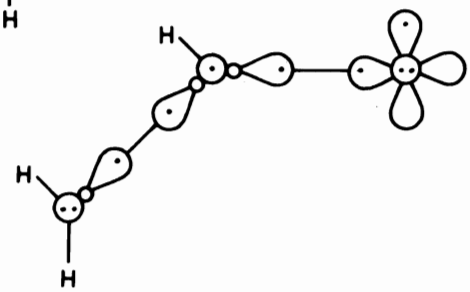

(5)

$^1A''$ and $^3A''$ for (5). From this valence bond model these states are expected to have charge distributions similar to those of the constituent atoms and will be referred to as *valence* states. The object of this paper will be to analyze the character of these states.

A fifth state, the $2^1A'(\pi \rightarrow \pi^*)$ state, will not be discussed in this paper. Since this state is expected to involve either charge-transfer character or a diffuse π^* orbital, it would not be well described with our valence basis set.

The above analysis of the formamide wave functions in terms of atomic orbitals is referred to as a valence bond analysis and diagrams such as in (1)–(5) are referred to as generalized valence bond diagrams. In the theoretical studies of this paper we have used the generalized valence bond (GVB) method[5,6] in which the orbitals of a valence bond-type wave function are solved for self-consistently. These results indicate that (3) and (4) correctly describe the qualitative nature of the states but readjustment effects are important for a good quantitative description.

The orbitals from the GVB calculations were also used in configuration interaction calculations which include some correlation and spin coupling effects omitted in the GVB wave function.

The details of the calculations are discussed in section II, a description of the GVB orbitals is contained in section III, and calculated excitation energies, dipole moments, and rotational barriers are discussed in section IV.

II. Calculational Details

A. Basis Set and Geometries. The double ζ (DZ) basis of Huzinaga[7] and Dunning[8] [(9s,5p/4s) primitive Gaussian contracted to (4s,2p/2s)] was used for all calculations.

The two geometries considered follow (see Figure 1). (a) R_{CO} = 1.193 Å, ∠N-C-H_a = 113.2°, R_{CN} = 1.376 Å, ∠C-N-H_b = 120.5°, R_{CH_a} = 1.102 Å, ∠C-N-H_c = 117.1°, R_{NH_b} = 1.002 Å, ∠N-C-O = 123.8°, R_{NH_c} = 1.014 Å. This corresponds approximately to the experimental ground state geometry,[9] the difference being that the experimental geometry is nonplanar (H_b and H_c being 7-10° out of the plane). This small difference is not expected to lead to a significant effect on any of the results.

(b) R_{CO} = 1.193 Å, ∠H_b-N-H_c = 105.9°, R_{CN} = 1.425 Å, ∠C-N-H_b = 112.1°, R_{CH_a} = 1.102 Å, ∠C-N-H_c = 112.1°, R_{NH_b} = 1.011 Å, ∠O-C-N = 123.8°, R_{NH_c} = 1.011 Å, ∠N-C-H_a = 113.2°. This represents our guess for the geometry of the twisted ground state molecule (allowing the bonds about the N to be nonplanar as in NH_3).

B. The GVB Calculations. First we examine the HF wave function of NH_2CHO and consider the process of breaking the C-N bond, to form NH_2 and CHO. For NH_2CHO the HF wave function consists of 12 doubly occupied orbitals. For the separated species it consists of 11 doubly occupied orbitals and two singly occupied orbitals. Therefore the HF wave function cannot properly describe this or any other process that involves forming or breaking two-electron bonds.

In the full GVB wave function every electron is allowed to have its own orbital, leading, in the case of formamide, to 24 orbitals. However, for the purpose of describing the valence states, the valence bond model (4) and (5) indicates that only three HF pairs must be allowed to split into nonorthogonal singly occupied orbitals. We will use the notation GVB(3) to denote that only three pairs are being described in terms of singly occupied orbitals. Of course, all 15 orbitals are solved for self-consistently. In addition, in our calculations we restrict the GVB(3) wave function by dividing the singly occupied orbitals into mutually orthogonal singlet- or triplet-coupled pairs (referred to as the perfect pairing approximation). To indicate this restriction we use the symbol PP. Thus the GVB(3/PP) wave function of formamide is of the form,

$$\mathcal{A}\{[\phi_1^2\phi_2^2\cdots\phi_9^2\alpha\beta\cdots\alpha\beta](\phi_{10}\phi_{11} + \phi_{11}\phi_{10})(\alpha\beta - \beta\alpha)(\phi_{12}\phi_{13} + \phi_{13}\phi_{12})(\alpha\beta - \beta\alpha)(\phi_{14}\phi_{15} \pm \phi_{15}\phi_{14})(\alpha\beta \mp \beta\alpha)\} \quad (6)$$

C. The CI Calculations.[10,11] Wave functions of the valence bond form,

$$\phi_a\phi_b + \phi_b\phi_a$$

with ϕ_a and ϕ_b being nonorthogonal, may be transformed to an equivalent natural orbital (NO) representation,

$$c_1\phi_1^2 - c_2\phi_2^2$$

where the NO's, ϕ_1, and ϕ_2 are orthogonal. In general the first natural orbital of a GVB bonding pair (the one with the dominant coefficient) may be interpreted as a bonding orbital and the second as an antibonding or correlating orbital.

The GVB-CI results reported here are most simply described by considering the three sets of orbitals, A, CN (σ,σ^*); B, CO (σ,σ^*); C, CO (π,π^*), 1a″.

Up to quadruple excitations were allowed within the space A + B + C under the restriction that there be no excitations between sets. Thus, for example, we would include configurations a-c but not d.

In addition to these configurations, for the A″ states we allowed excitations into the singly occupied a′ orbital from the a′ occupied space coupled with any single excitation within the entire occupied space (with the exception of the 1s orbitals). This type of CI calculation was, in the case of formaldehyde, found to be sufficient for calculating valence state excitation energies.

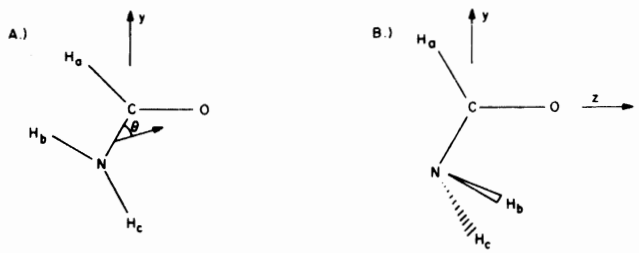

Figure 1. The geometries of NH_2CHO used in the calculations.

	σ_{CN}	σ^*_{CN}	σ_{CO}	σ^*_{CO}	π_{CO}	π^*_{CO}	1a″
a	2	0	2	0	2	0	2
b	1	1	1	1	1	1	2
c	0	2	2	0	2	1	1
d	2	2	0	0	2	0	2

These calculations, referred to as GVB-CI, partially relax the perfect pairing restriction and include the major correlation effects neglected in the GVB wave functions.

III. The GVB Orbitals

A. The Ground State. The ground state GVB(3) orbitals are shown in Figures 2 and 3. Although these orbitals are allowed to delocalize over the molecule, we find that they localize in different regions and have the basic character of the VB wave functions. This is clearly of great assistance in providing an intuitive feel for such chemical concepts as bonding and nonbonding pairs and bond polarities.

In the σ system of the molecule (Figure 2), we find three basic types of bonding pairs in addition to two nonbonding pairs on the oxygen atom.

The first type of bonding pair is the CO σ bond consisting of one orbital centered on oxygen hybridized toward the carbon and a second orbital centered on carbon but showing a large shift toward the oxygen.

Similarly, the second type of bonding pair forms the C-N bond. The orbital centered on the carbon is shifted toward the nitrogen, resulting in the N^-C^+ polarity of the bond. Overlaps and energy lowerings for these pairs are summarized in Table I.

The remaining bond pairs, which are not split in the GVB(3) wave function, correspond to the C-H and N-H bonds. Here, since the orbitals are doubly occupied, they are not unique. Any nonsingular transformation of them will not change the energy. These orbitals, however, do turn out to be well localized in the C-H and N-H region of the molecule.

The remaining two σ orbitals, which are also not split in the GVB(3) wave function, clearly represent the 2s and $2p_y$ nonbonding pairs of oxygen. These orbitals are nonunique but show a remarkable degree of localization.

Previous HF calculations[14] have led to an extremely delocalized lone pair orbital for the ground state and a relatively localized lone pair orbital for the n → π^* states. This has been interpreted by Robin[24] to indicate stabilization of oxygen → carbon charge-transfer character in these states. Our results indicate that the delocalized nature of the ground state HF lone pair orbital is simply an artifact of the HF calculation. Such behavior is not surprising since the orbitals resulting from a closed shell HF calculation are not "energy unique", i.e., any orthogonal transformation

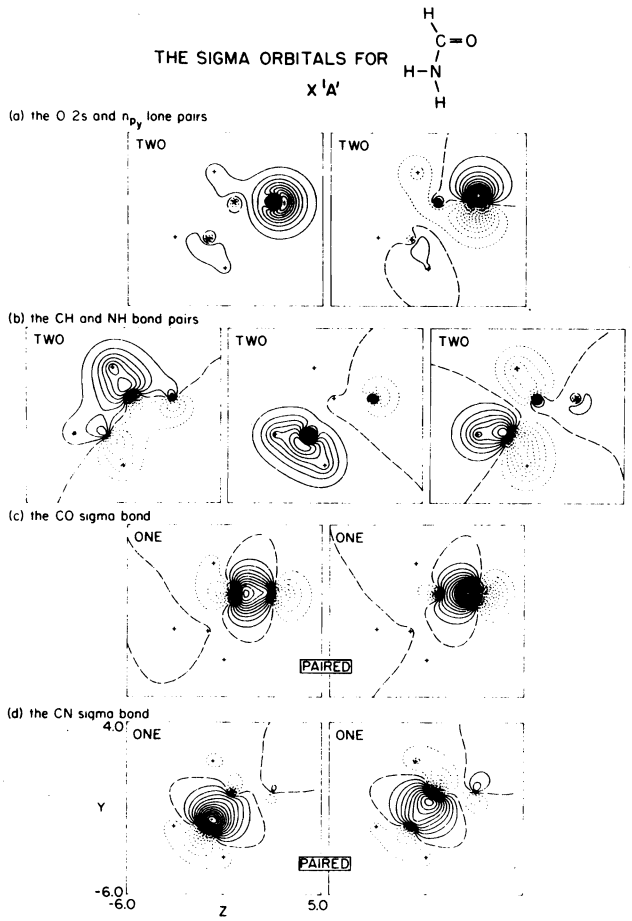

Figure 2. The ground state GVB(3) σ orbitals of planar NH_2CHO. The 1s orbitals are not shown. Long dashes indicate zero amplitude; the spacing between contours is 0.05 au. The same conventions are used for all plots.

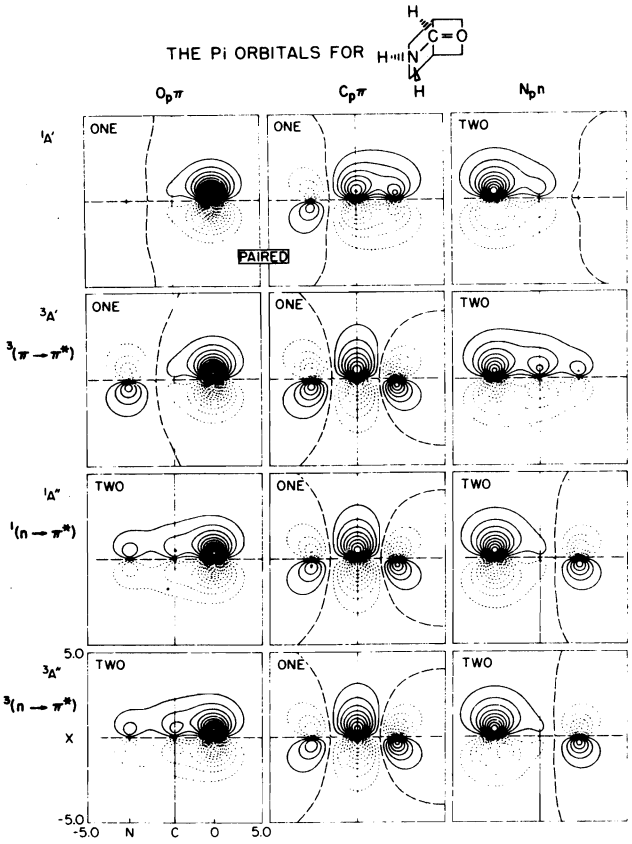

Figure 3. The GVB(3) π orbitals of the valence states of planar NH_2CHO.

Table I. Energies and GVB Parameters for the GVB(3) Wave Functions of NH_2CHO (All Quantities in au)

State	Geometry[a]	Total E	Pair Information		
			Pair	Overlap	ΔE,[b] hartrees
$^1A'$	A	−168.94352	CO σ	0.864	0.0144
			CN σ	0.849	0.0144
			CO π	0.689	0.0325
	B	−168.92094	CO σ	0.866	0.0141
			CN σ	0.830	0.0165
			CO π	0.650	0.0395
$^3A'(\pi \rightarrow \pi^*)$	A	−168.72768	CO σ	0.867	0.0139
			CN σ	0.852	0.0139
	B	−168.70776	CO σ	0.868	0.0138
			CN σ	0.831	0.0164
$^1A''(n \rightarrow \pi^*)$	A	−168.74422	CO σ	0.868	0.0139
			CN σ	0.858	0.0131
	B	−168.75328	CO σ	0.869	0.0137
			CN σ	0.845	0.0144
$^3A''(n \rightarrow \pi^*)$	A	−168.75522	CO σ	0.868	0.0139
			CN σ	0.859	0.0130
	B	−168.76599	CO σ	0.869	0.0136
			CN σ	0.845	0.0144

[a] See Figure 1. [b] Energy increase upon replacing the GVB pair by a HF pair (averaging the GVB orbitals to obtain the HF orbital).

among them will not affect the energy. In the GVB calculations, this nonuniqueness has been, to a large extent, removed and hence we find that the lone pair orbitals of all the valence states are well localized.

The π system of the GVB(3) wave functions (Figure 3) consists of two singly occupied orbitals and one doubly occupied orbital. The singly occupied orbitals represent the C–O π bond, one being centered on the oxygen and the other primarily on the carbon, but delocalized in a bonding way onto the oxygen and in an antibonding way onto the nitrogen. The remaining orbital is the nitrogen lone pair which is seen to have some C–N bonding character.

B. The Excited States. 1. π System. As expected from the GVB diagrams (4) and (5), the orbitals of the excited states are quite similar to those of the ground state with the most drastic changes occurring in the π system as shown in Figure 3.

In the $^3(\pi$–$\pi^*)$ state we find the lone pair to be highly delocalized in a bonding way over all three centers, while the two triplet-paired orbitals are highly delocalized in an antibonding way over all three centers.

The π orbitals of the A″ states are very similar, differing only slightly in the amount of delocalization of the singly occupied orbital (the triplet being more delocalized onto the oxygen). This is in exact analogy to our findings in formaldehyde although the effect here is not quite as great.

2. σ System. We find that the four valence states of formamide all involve very similar σ systems. This is expected from the valence bond description of the states, (3) and (4).

As in formaldehyde,[4] we find the singly occupied lone-pair orbital of the $^3A''$ state to be slightly more delocalized than that of the $^1A''$ state. This is, again, undoubtedly due to the exchange interaction with the singly occupied π orbital.

C. The Twisted Geometry. The a″ orbitals for the four valence states at geometry B (the twisted geometry) are shown in Figure 4. The most important difference between these orbitals and those of geometry A is the degree of lo-

Table II. Comparison of Vertical Excitation Energies in CH_2O and NH_2CHO

	NH_2CHO			CH_2O		
	GVB(3)	GVB-CI	Exptl	GVB(2)[a]	GVB-CI[a]	Exptl
$^3(\pi-\pi^*)$	5.91	6.19		5.41	5.95	6.0[c]
$^1(n-\pi^*)$	5.43	5.65	5.65[b]	3.91	4.09	4.1[d]
$^3(n-\pi^*)$	5.14	5.39		3.54	3.62	3.5[c]

[a] L. B. Harding and W. A. Goddard III, ref 4. [b] H. Basch, M. B. Robin, and N. A. Kuebler, ref 14. [c] A. Chutjian, ref 15. [d] M. J. Weiss, C. E. Kuyatt, and S. Mielczarek, ref 16.

calization. At geometry B all of the unique orbitals are well localized into either the carbonyl region or the NH_2 region. This effect is most evident in the $^3A'$ state where for the planar geometry the nitrogen lone pair is delocalized in a bonding way over all three centers, whereas at the twisted geometry the N–H a″ orbital is almost as localized as the $^1A'$ orbital. This difference in the degree of bonding delocalization is undoubtedly the primary cause of the high rotational barrier for these states (see Discussion, section C).

IV. Discussion

A. Excitation Energies. 1. Results. The calculated vertical excitation energies are listed in Table II and are compared with the few experimental results. The calculated $^1A''(n-\pi^*)$ vertical excitation energy corresponds closely with the peak in the absorption spectrum just as for formaldehyde (where both $n-\pi^*$ vertical excitation energies were found to be within 0.1 eV of the corresponding peaks in the absorption spectrum).

There has been some discussion in the literature concerning the nature of the lowest triplet state of peptide groups in general and of formamide in particular. On the basis of approximate calculations, Pullman[22] has concluded that the lowest triplet state of formamide is the $^3(n \rightarrow \pi^*)$. More recently, however, McGlynn[23] has suggested corrections to the Pullman calculations that invert the ordering of the $^3(n \rightarrow \pi^*)$ and $^3(\pi \rightarrow \pi^*)$ states. McGlynn[23] has also reported an approximate calculation on *N*-methylacetamide, predicting the lowest triplet state to be the $^3(\pi \rightarrow \pi^*)$ state.

Basch, Robin, and Kuebler[14] have reported indirect SCF and CI calculations on formamide. Their BADZ-CI calculations predicted the $^3(\pi \rightarrow \pi^*)$ state to be 0.4 eV below the $^3(n \rightarrow \pi^*)$ state while their BADZ-SCF results predicted the reverse ordering.

Our ab initio calculations show quite conclusively that the lowest triplet state of formamide is the $^3(n \rightarrow \pi^*)$ state, lying approximately 0.7 eV below the $^3(\pi \rightarrow \pi^*)$ state. These conclusions are in contradiction to the results of McGlynn and of Basch et al. mentioned above.

In Table II we compare the formamide excitation energies with those of formaldehyde in order to determine the effects of the NH_2 substituent on the energies of the states. Both $(n-\pi^*)$ excitation energies are approximately 1.6 eV higher than for formaldehyde. However, the $^3(\pi-\pi^*)$ excitation energy is only 0.2 eV higher. These results indicate that the lone pair significantly destabilizes the $(n-\pi^*)$ states but not the $^3(\pi-\pi^*)$ state (relative to the corresponding states in CH_2O). The reason for this effect can be seen clearly in the orbital plots of the π system (Figure 2). In the $^3(\pi-\pi^*)$ state the lone pair is delocalized in a bonding way whereas in the $(n-\pi^*)$ states the other doubly occupied π orbital prevents this so that the lone pair develops antibonding character.

2. Comparison between Theoretical Values. The dominant configurations for the GVB-CI wave functions are listed in Table III, along with their energy contribution (defined as the energy loss upon deleting the configuration but without readjusting the remaining coefficients).

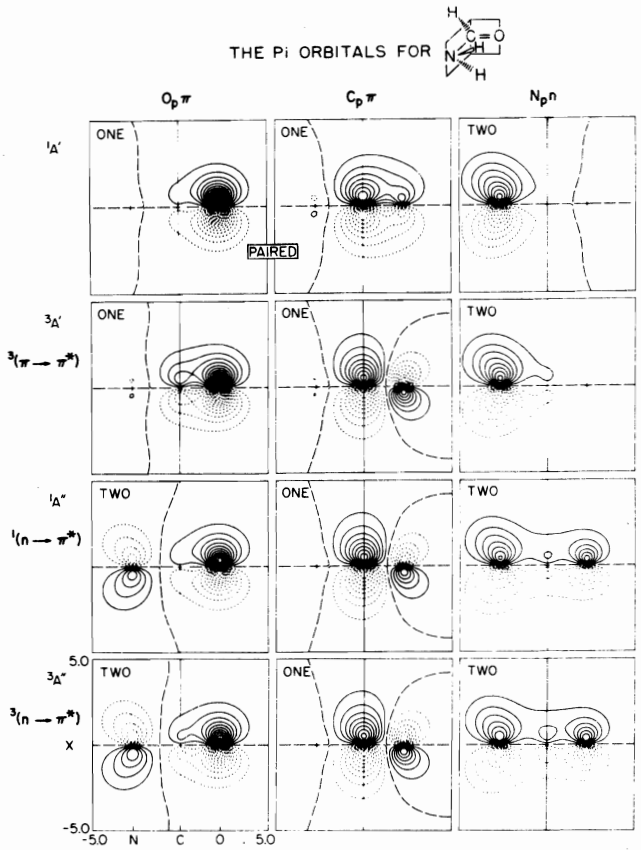

Figure 4. The GVB(3) π orbitals of the valence states of twisted (geometry B) NH_2CHO.

The major correlations included in the GVB-CI wave functions but neglected in the GVB(3) wave functions are the interpair correlations (the most important of these being between σ and π pairs).

In formaldehyde we found these correlations to be very important (~0.5 eV) for the ground state, but relatively unimportant for the valence excited states. This would have led to a ~0.5 eV error in all the GVB(2) excitation energies, except that in the $(n-\pi^*)$ states there is a cancelling error resulting from the neglect of $CH_{b_2} \rightarrow \pi^*$ excitations. The result is that the GVB(2) calculations lead to excellent $n-\pi^*$ excitation energies but a $^3(\pi-\pi^*)$ excitation energy ~0.5 eV below the GVB-CI results.

In formamide we find all of the GVB(3) excitation energies to be within ~0.25 eV of the GVB-CI results (see Table II). For the $n-\pi^*$ states the explanation of this agreement is essentially the same as in CH_2O. For the $^3(\pi-\pi^*)$ state we find that the highly delocalized bonding nature of the a″ lone pair causes a σ-lone pair interpair correlation effect ($\sigma_{CN} \rightarrow \sigma^*_{CN}, n \rightarrow \pi^*$) and ($\sigma_{CO} \rightarrow \sigma^*_{CO}, n \rightarrow \pi^*$) of 0.4 eV. This effect approximately cancels the CO $\sigma-\pi$ correlation in the ground state leading to the good agreement of the GVB(3) and GVB-CI excitation energies.

B. Dipole Moments. We find excellent agreement between the GVB(3) dipole moment (3.79 D) and the experimental number (3.71 D).[13] This is in sharp contrast to previously reported HF dipole moments (4.95 and 4.14 D).[14,20] We also find the orientation of the GVB(3) dipole moment (θ = 42.5°, see Figure 1) to be in good agreement with experiment (θ = 39.6°)[13] and previous HF calculations (θ = 42.1 and 42.6°).[14] The calculated dipole moment orienta-

Table III. Summary of Important Contributions[a] to the GVB-CI Wave Functions

A. A′ States

	Configuration CO $\sigma\sigma^*$	CN $\sigma\sigma^*$	CO $\pi\pi^*$	1a″	Character	Energy contributions,[b] mhartrees[c] Geometry A	Geometry B
^{1}A′	2 0	2 0	2 0	2	GVB		
ground	2 0	2 0	0 2	2	GVB	24.6	30.4
state	2 0	1 1	1 1	2	$\sigma \rightarrow \sigma^*, \pi \rightarrow \pi^*$	22.6	22.7
	0 2	2 0	2 0	2	GVB	13.2	16.1
	2 0	0 2	2 0	2	GVB	10.9	10.6
	1 1	2 0	2 1	1	$\sigma \rightarrow \sigma^*$, 1a″ $\rightarrow \pi^*$	7.6	1.4
	2 0	0 2	0 2	2	GVB	1.2	1.5
	2 0	2 0	2 2	0	$(1a'')^2 \rightarrow (\pi^*)^2$	1.1	0.1
^{3}A′$^3(\pi-\pi^*)$	2 0	2 0	1 1	2	GVB		
	2 0	0 2	1 1	2	GVB	13.3	13.8
	0 2	2 0	1 1	2	GVB	11.6	16.3
	1 1	2 0	1 2	1	$\sigma \rightarrow \sigma^*, n \rightarrow \pi^*$	8.4	0.9
	1 1	2 0	2 1	1	$\sigma \rightarrow \sigma^*, n \rightarrow \pi$	7.3	1.1
	2 0	1 1	2 1	1	$\sigma \rightarrow \sigma^*, n \rightarrow \pi$	2.8	~0.0
	2 0	2 0	1 2	1	π readjustment	1.7	~0.0
	2 0	1 1	1 2	1	$\sigma \rightarrow \sigma^*, n \rightarrow \pi^*$	1.6	0.2
	2 0	1 1	2 0	2	$\sigma \rightarrow \sigma^*, \pi^* \rightarrow \pi$	0.7	1.4

B. A″ States (n–π^*)

	Configuration CO $\sigma\sigma^*$	CN $\sigma\sigma^*$	CO $\pi\pi^*$	1a″	n	a′[d]	Character	Energy contributions,[b] mhartrees[c] Geometry A Singlet	Geometry A Triplet	Geometry B Singlet	Geometry B Triplet
	2 0	2 0	2 1	2	1	2	GVB				
	2 0	0 2	2 1	2	1	2	GVB	12.9	12.4	12.4	11.8
	0 2	2 0	2 1	2	1	2	GVB	12.4	12.3	14.4	14.1
	2 0	1 1	1 2	2	1	2	$\sigma \rightarrow \sigma^*, \pi \rightarrow \pi^*$	4.9	6.4	4.3	5.6
	1 1	2 0	2 2	1	1	2	$\sigma \rightarrow \sigma^*$, 1a″ $\rightarrow \pi^*$	4.2	3.2	1.0	1.0
	2 0	1 1	2 1	2	1	2	σ readjustment	2.8	1.0	2.6	1.0
	1 1	2 0	2 1	2	1	2	σ readjustment	2.8	0.9	5.2	1.6
	1 0	2 0	2 1	2	2	2	σ readjustment	1.4	1.1	2.6	1.6
	1 0	1 1	2 1	2	2	2	$\sigma \rightarrow \sigma^*, \sigma \rightarrow n$	1.3	1.2	1.8	1.7
	1 0	2 0	2 2	1	1	2	$\sigma \rightarrow n$, 1a″ $\rightarrow \pi^*$	1.2	1.0	0.4	0.4
	1 1	1 1	2 1	2	1	2	$\sigma \rightarrow \sigma^*, \sigma \rightarrow \sigma^*$	1.2	1.1	1.3	1.2
	2 0	1 1	1 2	2	1	2	$\sigma \rightarrow \sigma^*, \pi \rightarrow \pi^*$	1.2	1.2	0.0	0.1
	2 0	1 1	2 1	2	2	1	a′ $\rightarrow$ n, $\sigma \rightarrow \sigma^*$	1.0	1.2	1.3	1.6
	2 0	1 1	2 2	2	1	2	$\sigma \rightarrow \sigma^*$, 1a″ $\rightarrow \pi^*$	0.3	0.5	2.1	3.1
	1 0	2 0	1 2	2	2	2	$\sigma \rightarrow n, \pi \rightarrow \pi^*$	0.7	0.8	1.6	1.6
	0 1	2 0	2 1	2	2	2	$\sigma \rightarrow n, \sigma \rightarrow \sigma^*$	0.8	0.8	1.0	1.0
	2 0	2 0	1 2	2	2	1	a′ $\rightarrow$ n, $\pi \rightarrow \pi^*$	0.8	1.0	1.0	1.0

[a] All spatial configurations leading to an energy contribution larger than 1 mhartree are listed. [b] Each energy contribution listed here is the increase in the energy that would result from deleting this configuration without modifying the other CI coefficients. [c] The units here: mhartree = 10^{-3} hartree = 0.0272 eV = 0.63 kcal/mol.

Table IV. GVB(3) Orbital Components of the Dipole Moment (in au) for NH_2CHO at Geometry A

	σ system: Non-GVB[a]		σ system: CO σ pair		σ system: CN σ pair		π system: Non-GVB[b]		π system: GVB[c]		Total		$\lvert\mu\rvert$ Calcd		$\lvert\mu\rvert$ Exptl,	
State	y	z	y	z	y	z	y	z	y	z	y	z	au	Debye	D	θ[d]
^{1}A′	−0.350	0.022	−0.017	−0.647	0.322	0.192	−0.435	−0.268	0.127	−0.744	−0.353	−1.45	1.49	3.78	3.71	42.5
^{3}A′	−0.316	−0.082	−0.020	−0.678	0.391	0.217	−1.46	−1.24	0.668	0.715	−0.735	−1.06	1.29	3.28		21.5
^{1}A″	−0.412	0.341	0.048	−0.687	0.314	0.060	−0.363	0.120	0.126	0.034	−0.286	−0.814	0.863	2.19		36.8
^{3}A″	−0.396	0.377	0.048	−0.687	0.316	0.062	−0.338	0.297	0.111	−0.057	−0.261	−0.763	0.806	2.05		37.3

[a] C 1s, N 1s, O 1s, O 2s, NH_a, NH_b, CH, O 2p. [b] The orbitals labeled as TWO in Figure 3. [c] The orbitals labeled as either ONE or PAIRED in Figure 3. [d] See Figure 1.

tions for the excited states are $^3A'(\theta = 21.5°)$, $^1A''(\theta = 36.8°)$, and $^1A''(\theta = 37.3°)$.

One major advantage of the GVB wave functions is that since the important bonding orbitals are unique, it is possible to analyze a property such as the dipole moment in terms of orbital contributions. In order to do this consistently it is necessary to associate with each orbital contribution an appropriate nuclear contribution; for each electron we associate a unit nuclear charge centered at the nucleus on which the VB orbital is located (for example, we define the orbital contribution of the oxygen 2s lone pair as twice the orbital matrix element plus the contribution from a charge of 2+ centered on the oxygen).

Applying this analysis to the GVB(3) ground state wave function, we find (see Table IV) the CO σ, CO π, and CN σ bonds to all be strongly polar, shifting electron density away from the carbon. The other a′ orbitals (NH, CH, σ lone pairs) and the nitrogen lone pair, though, show a smaller shift in the opposite direction leading to the calculated dipole moment of 1.49 au (3.79 D).

We can also apply this analysis to the excited states in order to determine the effects of readjustments in the orbit-

Table V. Calculated Barriers to Rotation[a] about the C–N Bond (kcal)

	HF	GVB(3)	GVB-CI	Exptl
$^1A'$	24[c]	14.2	18.2	16–20[b]
$^3A'$		12.5	21.0	
$^1A''$		−5.7	−5.7	
$^3A''$		−6.5	−6.5	

[a] A negative sign indicates that the twisted geometry is more stable. [b] Liquid phase rotational barrier for the following solutions: neat, H_2O, acetone, dioxane, methyl propyl ketone, and diethylene glycol dimethyl ether are: 18.9, 21.3, 16.9, 16.8, 19.7, and 19.2, respectively (see ref 17, 18, and 19). [c] From ref 21.

als of the excited states. The results show that by far the most important changes occur in the π system (see Table IV).

For the $^3A'$ state the contribution of the nitrogen lone pair shows a large shift into the carbonyl region, as is indicated in the orbital plots. The two singly occupied π orbitals show a counter-balancing shift onto the nitrogen, resulting in a net decrease in the dipole moment.

The contributions for the $^1A''$ and $^3A''$ states are very similar. Here there are two doubly occupied π orbitals and hence there is a certain amount of non-uniqueness between them. The whole π system, though, shows a net decrease in its contribution (relative to the ground state), leading to a decrease in the total dipole moment of about 0.6 au (1.5 D).

C. Rotational Barriers. 1. Ground State. Barriers to rotation about the C–N bond were calculated for all four valence states and are summarized in Table V. The only experimental values available for comparison are the solution phase results for the ground state, also summarized in Table V. Of these the ones carried out in less polar solvents are expected to yield results closest to the gas phase barrier. We find excellent agreement between the calculated value (18.2 kcal) and the various relevant experimental values (16–20 kcal). Previous HF calculations on the rotational barrier have been reported and have been found to give barriers consistently too high (20–24 kcal).[20,21] We find this to be due primarily to an increase in the correlation energy in the π bond upon rotating the NH_2 group out of the plane (see Table I). Accounting for this effect alone lowers the rotational barrier by approximately 4 kcal.

2. Excited States. For the $^3A'(\pi \rightarrow \pi^*)$ state we find an *increase* in the rotational barrier of about 2.5 kcal with respect to the ground state. This is clearly consistent with the extreme bonding delocalization found for the nitrogen lone pair in the planar configuration.

For the $^1A''$ and $^3A''(n \rightarrow \pi^*)$ states we find the twisted geometry to be more stable by 5.7 and 6.5 kcal, respectively. This effect is no doubt due to the increased pair–pair repulsions in the π system. Note, however, that the twisted geometry has a nonplanar nitrogen center while the planar geometry has a planar nitrogen; for ammonia the barrier for such conversions is 6 kcal, numerically equal to the calculated barrier.

D. The Peptide Bond. For the ground state of formamide we find a sizable bonding delocalization of the nitrogen lone pair into the carbonyl region, leading to a calculated barrier to rotation about the C–N bond of 18.2 kcal. We expect similar interactions in the peptide bonds of proteins to be important in determining the preferred conformation of the protein molecules.

In the lowest-lying, singlet and triplet excited states, we find the twisted geometry to be approximately 6 kcal more stable than the planar geometry. Thus such excitations in a protein would lead to a disruption of the natural conformation of the protein but without affecting the sequence of amino acids within the protein (ignoring dissociation of the CN bond).

IV. Summary

The GVB wave functions lead to a consistent description of the valence states of formamide and the GVB orbitals provide simple explanations of the character of the states.

In addition, these orbitals form a very suitable basis for including the additional correlation effects necessary for a quantitative description with relatively small CI calculations.

Note Added in Proof. The trapped electron spectrum of formamide has recently been reported.[25] A feature was observed at 5.30 eV in excellent agreement with the calculated $^3(n \rightarrow \pi^*)$ excitation energy of 5.39 eV.

References and Notes

(1) Part of this work was carried out at the Health Sciences Computing Facility, UCLA, sponsored by the National Institutes of Health Special Resources Grant RR-3.
(2) Partially supported by a grant (GP-40783X) from the National Science Foundation and by the donors of the Petroleum Research Fund, administered by the American Chemical Society.
(3) Earle C. Anthony Foundation Fellow and Blanche Mowrer Memorial Fund Fellow, 1973–1974.
(4) L. B. Harding and W. A. Goddard III, *J. Am. Chem. Soc.*, **97**, preceding paper in this issue (1975).
(5) P. J. Hay, W. J. Hunt, and W. A. Goddard III, *J. Am. Chem. Soc.*, **94**, 8243 (1972).
(6) W. A. Goddard III, T. H. Dunning, Jr., W. J. Hunt, and P. J. Hay, *Acc. Chem. Res.*, **6**, 368 (1973).
(7) S. Huzinaga, *J. Chem. Phys.*, **42**, 1293 (1965).
(8) T. H. Dunning, Jr., *J. Chem. Phys.*, **53**, 2823 (1970).
(9) C. C. Costain and J. M. Dowling, *J. Chem. Phys.*, **32**, 158 (1960).
(10) The CI calculations were carried out with the Caltech CI program (Bobrowicz,[11] Winter and Ladner,[12] and Moss, Harding, Walch, and Goddard).
(11) F. Bobrowicz, Ph.D. Thesis, California Institute of Technology, 1974.
(12) R. C. Ladner, Ph.D. Thesis, California Institute of Technology, 1971.
(13) R. J. Kurland and E. B. Wilson, Jr., *J. Chem. Phys.*, **27**, 585 (1957).
(14) H. Basch, M. B. Robin, and N. A. Kuebler, *J. Chem. Phys.*, **47**, 1201 (1967).
(15) A. Chutjian, *J. Chem. Phys.*, **61**, 4279 (1974).
(16) M. J. Weiss, C. E. Kuyatt, and S. Mielczarek, *J. Chem. Phys.*, **54**, 4147 (1971).
(17) B. Sunners, L. H. Pietto, and W. G. Schneider, *Can. J. Chem.*, **38**, 631 (1960).
(18) H. Kamei, *Bull. Chem. Soc. Jpn.*, **41**, 2269 (1968).
(19) T. Drakenburg and S. Forsen, *J. Phys. Chem.*, **74**, 1 (1970).
(20) D. H. Christensen and R. W. Kortzeborn, *J. Chem. Phys.*, **53**, 3912 (1970).
(21) L. Radom, W. A. Lathan, W. J. Hehre, and J. A. Pople, *Aust. J. Chem.*, **25**, 1601 (1972).
(22) A. Pullman, "Modern Quantum Chemistry", Part III, O. Sinanoglu, Ed., Academic Press, New York, N.Y., 1965, p 283.
(23) H. J. Maria, D. Larson, M. E. McCarille, and S. P. McGlynn, *Acc. Chem. Res.*, **3**, 368 (1970).
(24) M. B. Robin, "Higher Excited States of Polyatomic Molecules", Vol. II, Academic Press, New York, N.Y., 1975, p 128.
(25) R. H. Staley, L. B. Harding, W. A. Goddard III, and J. L. Beauchamp, *Chem. Phys. Lett.*, in press.